Copper(II)-mediated N-terminal modification of proteins with maleimide derivatives

Authors

Kengo Hanaya,[1]* Kazuaki Taguchi,[1] Yuki Wada,[2] Masaki Kawano,[2] and Shuhei Higashibayashi[1]

[1]Faculty of Pharmacy, Keio University, 1-5-30 Shibakoen. Manato-ku, Tokyo 105-8512, Japan

[2]Department of Chemistry, School of Science, Tokyo Institute of Technology, 2-12-1 Ookayama, Meguro-ku, Tokyo 152-8550 Japan

E-mail: hanaya-kn@keio.jp

Abstract

Maleimide derivatives are privileged reagents for the chemical modification of proteins via the Michael addition of cysteine due to their selectivity, reaction rate, and commercial availability. Since accessible free cysteine is rarely found in natural proteins, an alternative target for maleimide derivatives is highly desirable for direct bioconjugation. In this study, we developed a copper(II)-mediated [3+2] cycloaddition reaction with maleimide and 2-pyridinecarboxaldehyde (2-PC) derivatives as an operationally simple and powerful method for the N-terminal modification of peptides and proteins. This method utilizes commercially available maleimides to attach diverse functionalities to various N-terminal amino acids. The combined use of copper(II) ions and heteroaromatic aldehydes is key to the selective formation of azomethine intermediates at the N-terminus in aqueous media under mild conditions, achieving high N-terminal selectivity. We demonstrate the preparation of a ternary protein complex cross-linked at the N-termini and dually modified trastuzumab equipped with monomethyl auristatin E (MMAE), a cytotoxic agent, and a Cy5 fluorophore (MMAE–Cy5–trastuzumab). The MMAE–Cy5–trastuzumab retained human epidermal growth factor receptor 2 (HER2) recognition activity and exerted cytotoxicity against HER2-positive cells. Furthermore, MMAE–Cy5–trastuzumab helped successfully visualize HER2-positive cancer cells in mouse tumors. This straightforward method will enhance the accessibility and utility of protein conjugates with defined structures across a diverse spectrum of researchers.

Introduction

Bioconjugation reactions for protein modification enable the crosslinking of proteins with synthetic molecules and biopolymers, facilitating the labeling and creation of novel functionalized proteins not found in nature.[1–3] These reactions have been continually developed to meet the increasing demand in various fields, including activity-based protein profiling,[4–8] N-terminomics,[9,10] investigations into cellular processes,[11,12] fabrication of protein–biomolecule complexes and biopolymer-based materials,[13,14] and preparation of advanced biopharmaceuticals.[15–17] Ensuring a conjugate with uniform structure and properties requires precise control over the protein's reaction site and the number of attached molecules, even under mild pH and temperature conditions in aqueous solutions. To address this challenge, researchers have explored the chemical modification of rare canonical amino acids such as

cysteine,[18–22] tyrosine,[23–28] tryptophan,[29–33] methionine,[34–36] N-terminus,[37,38] and C-terminus,[39] as well as the genetic incorporation of non-canonical amino acids with bioorthogonal handles[40] or polypeptide tags[41–44] as unique reactive sites. Among these approaches, direct single-site chemical modification of canonical amino acids is particularly attractive due to its simplicity and convenience. Remarkable progress has been made in the chemical modification of specific amino acids in proteins of interest. However, despite these advancements, achieving high chemo- and/or site-selectivity often requires elaborately synthesized reagents with unique structures and finely tuned reaction conditions, limiting their widespread application by non-chemists in various fields. In this context, cysteine modification via Michael addition with maleimide derivatives remains the gold standard due to its high selectivity, operational simplicity, and the wide availability of maleimide derivatives.[45,46] Currently, various maleimide derivatives with specialized functional groups, such as photoactive groups, fluorophores, affinity tags, bioorthogonal handles, spin labels, pharmaceuticals, and hydrophilic solubilizing agents, are commercially available. However, accessible free cysteine is rarely found in the proteins of interest. Therefore, developing simple and reliable alternative methods using readily accessible maleimide derivatives to modify other amino acids could have a widespread impact across various scientific fields.

Azomethine ylide, derived from amino acids and arylaldehyde, is regarded as a bio-relevant 1,3-dipolar species that undergoes [3+2] cycloaddition with 1,3-dipolarophiles such as maleimide, vinylsulfone, and maleate to yield substituted pyrrolidines (Fig. 1a).[47–53] Recently, Kanemoto et al. successfully achieved N-terminal modification of peptides in an organic solvent using the copper(I)-catalyzed [3+2] cycloaddition of azomethine ylide with maleimides,[54] though the applicable amino acids at the N-terminus were limited. If azomethine ylides can be constructed on various N-terminal amino acids of proteins under biocompatible conditions, the [3+2] cycloaddition of azomethine ylides with maleimides would be a promising approach for the selective N-terminal modification of proteins. However, despite the long history of [3+2] cycloaddition of azomethine ylides, no examples of protein modification exist, likely due to several challenges. These include the low stability of amino acid imines in aqueous conditions and the requirement for basic conditions to generate azomethine ylides *in situ* via the deprotonation of the amino acid imine. Furthermore, substituted amino acids are less reactive precursors of azomethine ylides due to lower acidity of the α-proton by inductive effect and inefficient imine formation due to steric hindrance, resulting in a limited substrate scope of amino acids under conventional reaction conditions.[51] Indeed, most studies used glycine-derived imino esters, with few examples involving other amino acids such as alanine, leucine, phenylalanine, tryptophane, methionine, and tyrosine.[54,55] Therefore, the N-terminal modification of proteins with various N-terminal amino acids via [3+2] cycloaddition of azomethine ylide requires a strategy to enhance both imine formation and deprotonation of the α-proton.

We have recently reported the selective N-terminal modification of peptides and proteins with various N-terminal amino acids via copper(II)-mediated aldol reaction with pyridine-2-carboxaldehyde (2-PC) derivatives at a neutral pH and 37°C (Fig. 1b).[56] The copper(II) ion forms a stable ternary complex **I** with the Schiff base of the N-terminal amino acid and 2-PC, even in aqueous media. Due to the Lewis acidity of the metal ion, deprotonation of the α-proton occurs at neutral pH, generating a copper(II) enolate **II** *in situ*. Intermediate **II** reacts with 2-PC to afford the

aldol product after the decomposition of the Schiff base–copper(II) complex. Lysine also forms a Schiff base–metal complex on its side chain, which is inert during this process due to its low acidity. Lysine is regenerated after quenching, resulting in selective N-terminal modification.

We expect the *in situ*-generated intermediate **II** to be a potential 1,3-dipolar species. Herein, we developed a copper(II)-mediated [3+2] cycloaddition reaction using 2-PC derivatives and commercially available maleimide derivatives as a powerful tool for selective N-terminal protein modification (Fig. 1c). The developed method efficiently modified a wide variety of peptides and proteins with various N-terminal amino acids by simply mixing all required reagents for a few hours at a weakly acidic pH of 6 and 37 °C.
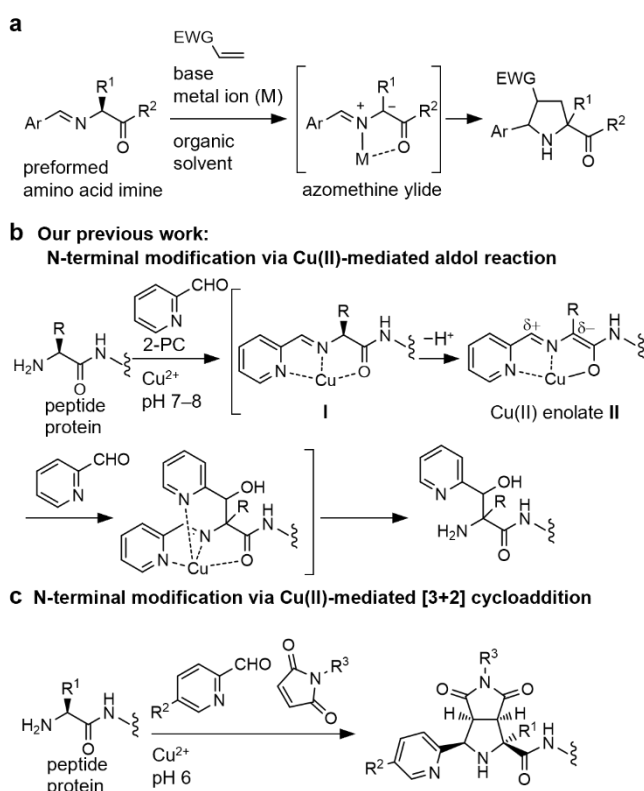

Fig. 1 N-termini as potential targets of maleimides. a General scheme of the [3+2] cycloaddition of azomethine ylide. **b** N-terminal modification of peptides and proteins via aldol reaction using *in-situ* generated copper(II) enolate. **c** N-terminal modification of peptides and proteins via copper(II)-mediated [3+2] cycloaddition.

Results and Discussion

As a model reaction, biologically active peptide T (**1**) was incubated with 2-PC (**2a**) and *N*-ethylmaleimide (**3a**) in the presence of Cu(OAc)$_2$ at 37°C in various buffers at pH 6 (Fig. 2a). LC-MS analysis showed complete conversion in 3 hours, yielding the desired adduct, **4aa**, quantitatively (Fig. 2b). Two new peaks at retention times of 8.9 and 9.0 minutes with the same m/z of 1072 (ΔM = +214 amu) were observed in LC-MS, indicating that both peaks corresponded to the two diastereomers of **4aa** (Fig. 2c). As observed in previous literatures,[56] aza-Michael

addition adducts at the N-terminus with **3a** (ΔM = +125 amu) and aldol adducts with **2a** (ΔM = +107 amu and +196 amu) were strongly suppressed at acidic pH. The modification site in **4aa** was identified at the N-terminus by LC-MS/MS analysis (Supplementary Fig. 1). Further structural elucidation of adduct **4aa** was conducted using NMR (Supplementary Fig. 2—4, Supplementary Table 1). In the ^{1}H NMR spectra, a proton at the α-position of N-terminal alanine (δ 3.88–3.85 ppm) in 1 disappeared after modification. The methyl signal of alanine changed from a doublet (δ 1.32 ppm) in **1** to a singlet (δ 1.50 or 1.59 ppm) in **4aa**. HSQC and HMBC results indicated the presence of a quaternary carbon (67.3 ppm in ^{13}C NMR of **4aa**) at the N-terminal residue, suggesting a 1,3-dipolar cycloaddition at the N-terminus, as expected. To estimate the stereochemistry of **4aa**, alanine derivative ($\pm$)-**5**, the N-terminal substructure of **4aa**, was synthesized by copper(II)-mediated [3+2] cycloaddition of alanine amide with **2a** and **3a**. Single crystal X-ray analysis of ($\pm$)-**5** revealed the endo-configuration, suggesting that **4aa** was a diastereomeric mixture of the endo products (Fig. 2d). The copper(II)-mediated N-terminal modification of **1** with **2a** and **3a** progressed at pH 6.0–8.0 with negligible amounts of byproducts (Supplementary Fig. 5). To minimize the undesired aza-Michael reactions of lysine and N-terminal amino acids and copper(II)-mediated aldol reactions in further studies using larger peptides and proteins, we concluded that a weakly acidic pH of 6.0 is optimal. Kinetic studies showed that the conversion rate constant of **1** at pH 6.0 was estimated to be 5.5×10^4 M^{-3}·sec^{-1} based on a simplified model (Supplementary Fig. 6). In the kinetic studies, we observed aldol product formation when the relative concentration of **2a** to **3a** was increased, indicating that an excess amount of **3a** was key to obtaining **4aa** in a high yield (Supplementary Fig. 6d). The newly constructed substructure in adduct **4aa** remained stable at acidic and neutral pH or in the presence of TCEP, glutathione, and hydrogen peroxide at 37°C. Succinimide ring-opening hydrolysis was negligible after incubation for three days under these conditions (Supplementary Fig. 7). In contrast, succinimide ring-opening hydrolysis was complete at a basic pH within 5 minutes, resulting in a complex mixture after incubation for 1 day (Supplementary Fig. 8).
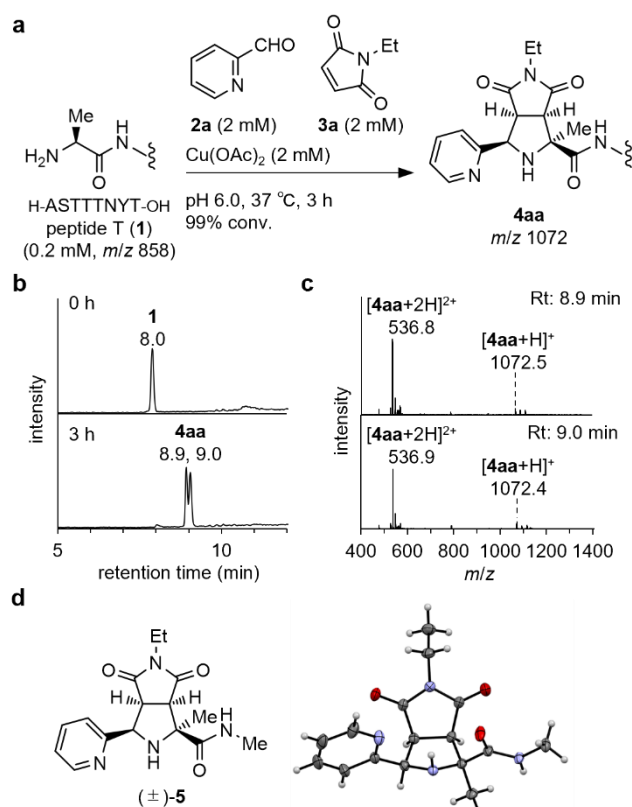
Fig. 2 Characterizations of the N-terminal conjugation. a N-terminal modification of peptide T (**1**) via copper(II)-mediated [3+2] cycloaddition with pyridine-2-carboxaldehyde (**2a**) and N-ethylmaleimide (**3a**). **b** Total ion chromatograms from LC-MS analyses of the crude reaction mixture of **1** with **2a** and **3a**. **c** Mass spectra of the fractions at 8.9 minutes and 9.0 minutes in LC-MS analysis. **d** The ORTEP diagram of (±)-**5**, the N-terminal substructure of **4aa** (probability level: 50%).

Other metal ions were examined as potential promoters of the N-terminal modification of **1** via [3+2] cycloaddition with **2a** and **3a** (Supplementary Fig. 9). In the presence of nickel(II) and cobalt(II) salts, **1** exhibited 96% and 88% conversion, respectively, forming various products through aldol reaction (ΔM = +107 amu), imidazolidinone formation (ΔM = +89 amu),[37] aza-Michael addition (ΔM = +125 amu), and transamination (ΔM = +28 amu). Interestingly, nickel(II) salt accelerated the aza-Michael addition of **1** and **3a**. Although silver(I)[57–60] and zinc(II)[61,62] salts are generally used in the [3+2] cycloaddition of azomethine ylides derived from substituted amino acids, the conversion of **1** were significantly low (<10%). Lewis acidity of these ions was insufficient to enhance both imine formation and deprotonation of the α-proton. Ultimately, we concluded that copper(II) salt provided the highest conversion of **1** (>95%), with **4aa** exclusively formed as the major product.

Subsequently, we assessed the conversion of **1** in reactions with other aryl aldehydes **2b–k** using LC-MS (Table 1, Supplementary Fig. 10 and 11). The modification reaction demonstrated strict requirements for aryl aldehydes

with adjacent coordination groups. Benzaldehyde (**2b**) and salicylaldehyde (**2c**) were unreactive, whereas heterocyclic aldehydes **2d–f** achieved high conversion and provided the corresponding adducts without noticeable byproducts. Pyridone-3-carboxaldehyde (**2f**) likely transformed *in situ* into the corresponding hydroxypyridine, which participated in the reaction. 8-Quinolinecarboxaldehyde (**2g**), capable of forming a six-membered chelation ring, produced the adduct, albeit with lower reactivity. 3-Pyridinecarboxaldehyde (**2h**), possessing a formyl group at the 3-position, resulted in negligible conversion, suggesting that the formation of a five-membered chelation ring at the N-terminus plays an important role in the [3+2] cycloaddition. Methyl-substituted 2-PCs **2i–k** were examined to determine the most favorable positions for introducing functionalities. Gratifyingly, the substituent position on the 2-PC ring had little impact on reactivity.

**Table 1.** Scope of aryl aldehyde on N-terminal modification of peptide T (**1**)
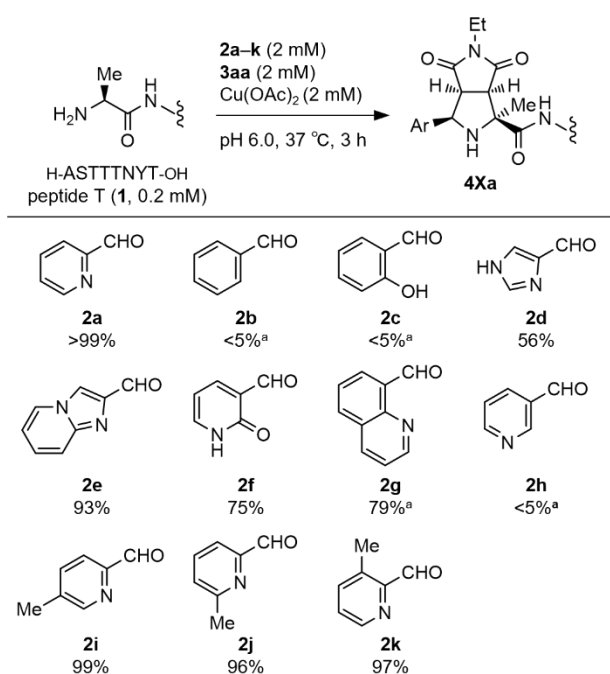
ᵃ Conversion of peptide T (**1**) after the reaction with various aryl aldehydes for 18 h.

1,3-Dipolarophiles **3a–e**, commonly used in bioconjugations, were screened for the copper(II)-mediated [3+2] cycloaddition of **1**. Among the tested compounds, *N*-ethylmaleimide (**3a**) and *N*-phenylmaleimide (**3b**) exhibited sufficient reactivity for practical applications (Table 2 and Supplementary Fig. 12). However, **3b** provided ring-opened adducts **4ab′**, produced via hydrolysis of the imide ring of **4ab**.[46] For **3c** and **3d**, which have poor reactivity, **1** is consumed by the copper(II)-mediated aldol reaction and successive imidazolidinone formation, producing a mixture of singly and doubly modified products of **2a**, as previously reported. Using **3e**, a complex mixture of unidentified products was obtained. Considering the reactivity and commercial availability of the functionalized derivatives, we conclude that *N*-alkylmaleimides are the most potent reagents for N-terminal modification via
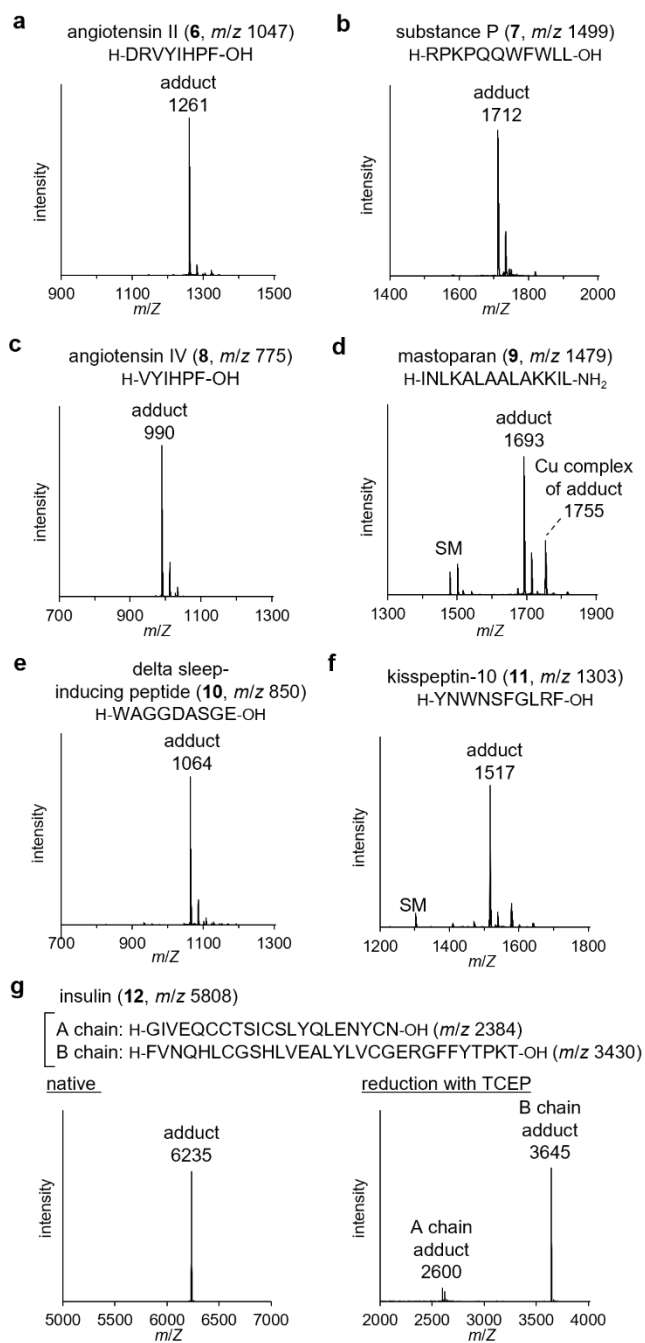
copper(II)-mediated [3+2] cycloaddition.

Table 2. Scope of dipolarophile on N-terminal modification of peptide T (**1**)
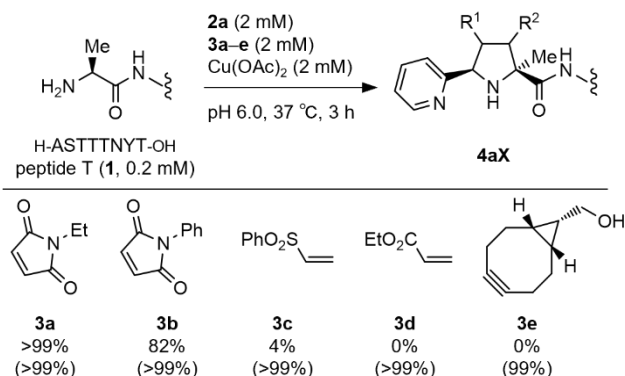
Conversion of peptide T (**1**) is shown in parentheses.

Copper (II)-mediated 1,3-dipolar cycloaddition with **2a** and **3a** enabled the modification of a wide range of biologically active peptides **6–12** with various N-terminal amino acids (Fig. 3 and Supplementary Fig. 13). The reactions provided the corresponding adducts without noticeable byproducts, as evidenced by MALDI-TOF MS and LC-MS analyses. For insulin (**12**), the N-termini of both the A and B chain were modified, resulting in doubly modified products (Fig. 3g). The N-terminal modifications of peptides **6–11** were confirmed by LC-MS/MS (Supplementary Fig. 14–19). N-terminal amino acids with charged, bulky, and aromatic side chains were compatible with the reaction. Even with multiple lysine residues capable of undergoing the aza-Michael reaction, specific modifications were observed at the N-terminus (Fig. 3d). In addition to the weakly acidic pH, which decreases the nucleophilicity of the lysine amino group of Lys, the amino group of lysine is transiently protected as a Schiff base–metal complex during the reaction, minimizing aza-Michael addition. Peptides with N-terminal metal-binding domains (His or Gly-Asn-His) showed significantly low reactivity. Pyroglutamic acid and N-acetylated amino acids at the N-terminus afforded no detectable adducts (Supplementary Fig. 20 and 21). These results strongly suggest the requirement for the formation of a ternary copper(II) complex.
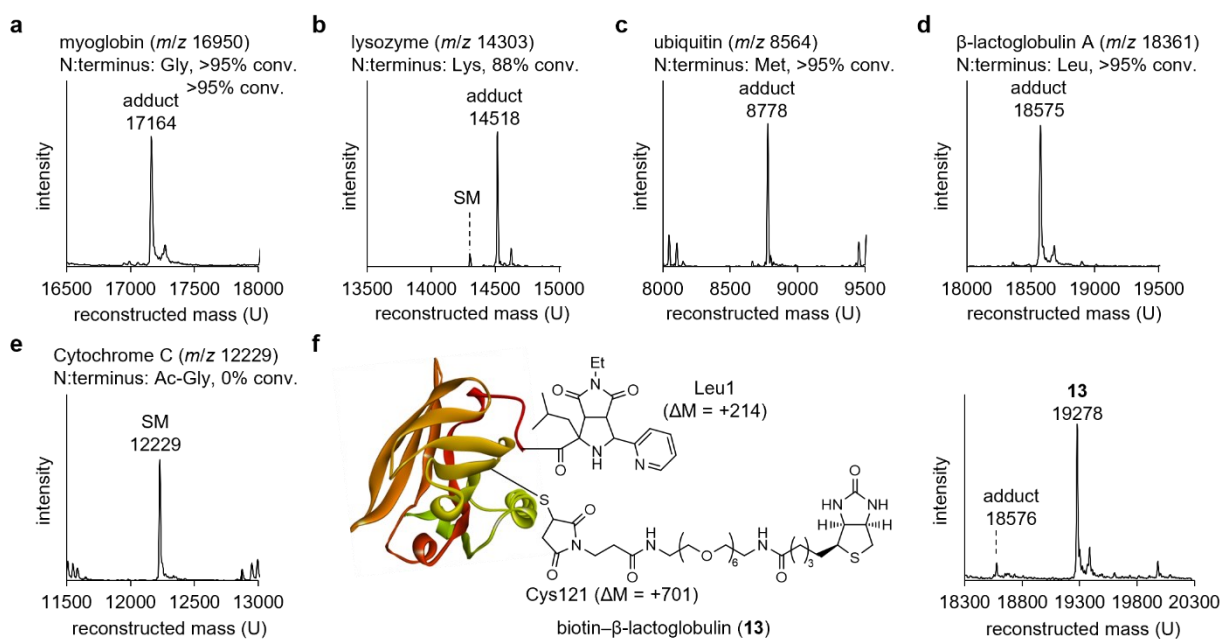
Fig. 3 Copper(II)-mediated [3+2] cycloaddition biologically active peptides with 2a and 3a. MALDI-TOF MS spectra of crude reaction mixtures. **a** Angiotensin II (**6**). **b** Substance P (**7**). **c** Angiotensin IV (**8**). **d** Mastoparan (**9**). **e** Delta sleep-inducing peptide (**10**). **f** Kisspeptin-10 (**11**). **g** Insulin (**12**). Conditions: peptides (0.2 mM), **2a** (2 mM), **3a** (2 mM), Cu(OAc)$_2$ (2 mM) in phosphate buffer (10 mM, pH 6.0) at 37 °C for 6 hours, then EDTA (4 mM) and methoxyamine (40 mM).

Copper (II)-mediated [3+2] cycloadditions can be used for protein modification. We performed modification reactions on myoglobin (N-terminus: Gly), lysozyme (N-terminus: Lys), ubiquitin (N-terminus: Met), β-lactoglobulin (N-terminus: Leu), and cytochrome C (N-terminus: Ac-Gly) with **2a** and **3a** (Fig. 4a–e). In all reactions, except for cytochrome C, high conversion of the parent protein was observed, and the expected conjugate (ΔM = +214) was detected as the major product (Fig. 4a–d). Tryptic digestion of each modified protein revealed that the modification occurred exclusively on the N-terminus-containing fragments (Supplementary Fig. 22–29). Cytochrome C, with an acetylated N-terminus, was unreactive, consistent with the peptide study (Fig. 4e). Notably, only a trace amount of the **3a** adduct resulting from the aza-Michael addition of lysine, was detected.

To assess the inhibitory effect of acidic pH and each reagent on the aza-Michael addition in protein modifications, reactions of cytochrome C and **3a** were conducted in the presence or absence of **2a** and copper(II) salt at pH 6.0 or 7.5 (Supplementary Fig. 30). The results revealed that both acidic pH and copper(II) ions contributed to the suppression of the aza-Michael addition. In particular, when both **2a** and copper(II) ions were used, the formation of the adduct with **3a** was most suppressed, even at pH 7.5, suggesting that lysine was transiently protected by forming a Schiff base–copper(II) complex during the reaction (Supplementary Fig. 30E and 30G).

Notably, β-lactoglobulin A was modified at the N-terminus despite the presence of one free cysteine (Cys121). Both the acidic pH and copper(II) ions inhibited cysteine modification with **3a** during the 1,3-dipolar cycloaddition (Supplementary Fig. 31). This allowed us to sequentially modify the N-terminal and Cys residues. The residual Cys121 was modified by 1,4-addition with biotin–PEG6–maleimide **14** at pH 7.5, forming the dually modified β-lactoglobulin A **13** (Fig. 4f).

**Fig. 4 Copper(II)-mediated [3+2] cycloaddition of proteins with 2a and 3a.** Deconvoluted mass spectra. **a** Myoglobin. **b** Lysozyme. **c** Ubiquitin. **d** β-Lactoglobulin. **e** Cytochrome C. **f** MALDI TOF-MS spectra of β-

lactoglobulin after sequential modification at N-terminal Leu (Leu1) and Cys121.

Functionalized 2-PC and maleimides were utilized for N-terminal modification. Trastuzumab, an anti-human epidermal growth factor receptor 2 (HER2) antibody used to treat metastatic breast cancer, reacted with biotinylated maleimide **14** and azide-2-PC **15** in the presence of copper(II) ions. After removing unreacted **14** and **15** using a desalting column, monomethyl auristatin E (MMAE), a microtubule inhibitor, was incorporated through click chemistry between azide and dibenzocyclooctyne (DBCO) using DBCO–PEG3–Glu–Val–Cit–PAB–MMAE (**20**). Despite the high molecular weight (~150 kDa) and complex structure of trastuzumab, MALDI-TOF MS analyses revealed that both the heavy chain (N-terminus: Glu) and light chain (N-terminus: Asp) were completely consumed and modified with one set of **14**, **15**, and **20** (theoretical $\Delta M = +2571$).

Introducing click chemistry to handle the N-terminus via 1,3-dipolar cycloaddition with commercially available maleimides **16–18** enabled the construction of cross-linked proteins with defined structures (Fig. 5c and 5d). Azide–tetrazine–β-lactoglobulin A (Az–Tet–Lac, **21**), DBCO–ubiquitin (DBCO–Ub, **22**), and trans-cyclooctene–myoglobin (TCO–Myo, **23**) were prepared using the developed method (Supplementary Fig. 32 and 33). The resulting conjugates were coupled to each other at their N-termini via strain-promoted azide-alkyne cycloaddition between azide and DBCO, and the inverse electron demand Diels-Alder reaction between tetrazine and cyclooctene. Formation of the binary conjugates Ub–Lac (**24**) and Lac–Myo (**25**) was confirmed by SDS-PAGE and size-exclusion column analyses. Furthermore, the ternary conjugate Ub–Lac–Myo (**26**) was successfully obtained by subsequent reactions of **24**, **23**, **25**, and **22** (Fig. 5e and Supplementary Fig. 34).
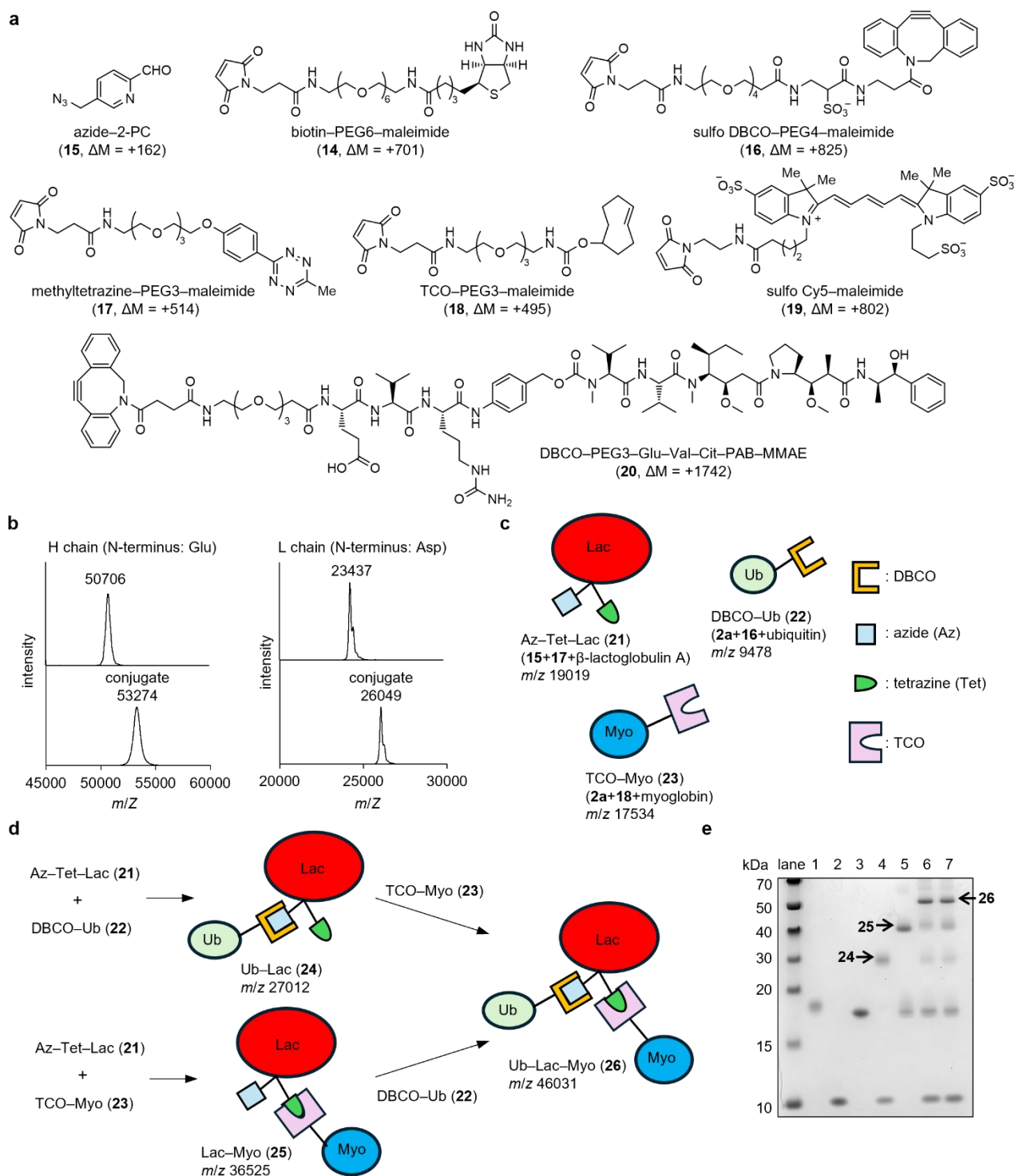
Fig. 5 N-terminal protein modification with functionalized maleimides. a Structures of reagents used in the experiments. **b** MALDI TOF-MS spectra of the heavy (H) chains and light (L) chains of trastuzumab (upper) and MMAE–biotin–trastuzumab (lower). **c** Schematic presentation of modified proteins with click chemistry handles. **d** The scheme for the sequential preparation of protein clusters **24**, **25**, and **26** by click chemistry. **e** Gel image of modified proteins and protein clusters. Lane 1: Az–tetrazine–Lac **21**; lane 2: DBCO–Ubi **22**; lane 3: TCO–Myo **23**;

lane 4: reaction mixture of **21** and **22**; lane 5: reaction mixture of **21** and **23**; lane 6: reaction mixture of **21**, **22**, then **23**; lane 7: the reaction mixture of **21**, **23**, and then **22**.

Next, we evaluated the compatibility of the N-terminal modification via copper(II)-mediated [3+2] cycloaddition with the intrinsic activity of the proteins. We prepared MMAE–Cy5–trastuzumab (**27**) via the copper(II)-mediated [3+2] cycloaddition of **15** and **19**, followed by a copper-free click reaction with DBCO–PEG3–Glu–Val–Cit–PAB–MMAE (**20**) (Fig. 6a and Supplementary Fig. 35). MMAE–Cy5–trastuzumab (**27**) was expected to not only visualize HER2-positive tumor cells but also release the active payload MMAE specifically at the tumor site upon cathepsin-mediated cleavage of the Glu–Val–Cit linker,[63] thereby treating cancer. The developed method provided **27** with an average of 3.0 molecules of MMAE and Cy5 molecules attached to the Fab regions of both the heavy and light chains, as demonstrated by UV-Vis. spectroscopy, MALDI-TOF MS, and in-gel fluorescence detection following papain treatment (Supplementary Fig. 36). We assessed the binding of **27** to HER2 on the cell surface by confocal microscopy (Fig. 6b and Supplementary Fig. 37). Although there was no significant fluorescent signal from HER2-negative human breast adenocarcinoma cells MCF-7, strong Cy5-derived fluorescent signals were observed on the surface of HER2-positive human gastric cancer cells NCI-N87. These results suggest that the N-terminal modification of trastuzumab had little impact on the structure of the antigen recognition site on the N-terminal domain. The anti-proliferative activity of **27** on MCF-7 and NCI-N87 cells was compared with that of the parent drugs, trastuzumab and MMAE, in 2D- and 3D-cultured models (Fig. 6c and 6d). While MMAE showed a non-specific inhibitory effect on both tumor cells in the 2D-cultured model, trastuzumab and **27** exhibited specific anti-proliferative activity only in HER2-positive NCI-N87 cells (Fig. 6c). Conjugate **27** displayed more potent activity than the parent drug, trastuzumab, at concentrations above 1 nM, comparable to that of MMAE. These results suggest that **27** did not release MMAE outside the cells but was internalized into the cells via HER2 receptor-mediated endocytosis to release MMAE into the cytosol through cathepsin-mediated hydrolysis of the Glu–Val–Cit linker. In the 3D culture model, trastuzumab did not affect the spheroid shape, whereas MMAE and conjugate **27** inhibited the growth of NCI-N87 spheroids and caused the spheroids to collapse (Fig. 6d and Supplementary Fig. 38). As the tumor spheroid mimics the *in vivo* tumor microenvironment,[64] the data from the 3D-cultured model strongly corroborate the potent anti-tumor activity of conjugate **27**. Finally, we assessed the biodistribution of **27** in NCI-N87-bearing mice by IVIS *in vivo* fluorescence imaging. MMAE–Cy5–trastuzumab (**27**) (0.22 mg/kg) was intravenously administered to the NCI-N87-bearing mice, and the fluorescent images were captured at the specified time points (Fig. 6e). The fluorescence signal of Cy5 was observed in the tumor at 3 hours after administration and continued to increase until 24 hours (Fig. 6e). Quantification of the fluorescent signals in the dissected organs indicated a high accumulation of **27** in the tumor tissue (Fig. 6f).
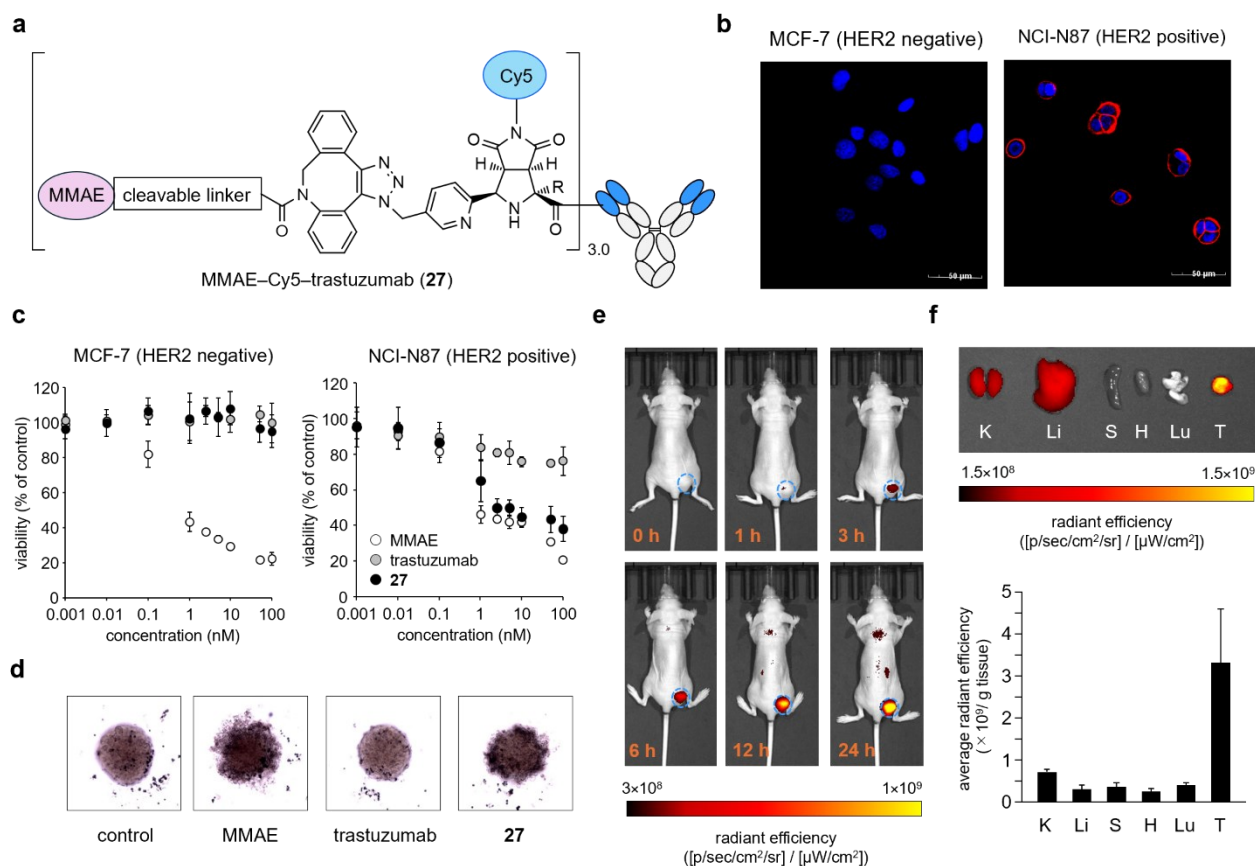
Fig. 6 Activity evaluation of MMAE–Cy5–trastuzumab (27). a Schematic view of MMAE–Cy5–trastuzumab **27**.
b Representative confocal microscopy images of human epidermal growth factor receptor 2 (HER2-positive cells
NCI-N87 cells and HER2-negative cells MCF-7 cells treated with **27** (red). Blue: nuclear stain with DAPI. Scale
bar: 50 μm. **c** Cytotoxicity assay of MMAE, trastuzumab, and **27** on HER2-positive NCI-N87 cells and HER2-
negative MCF-7 cells. Values on each bar represent the average cell viability from three independent experiments.
d Representative morphology of NCI-N87 spheroids treated with MMAE (10 nM), trastuzumab (3.5 nM), and **27**
(MMAE: 10 nM, trastuzumab: 3.5 nM). **e** Representative fluorescent images of the NCI-N87-bearing mice at 0, 1,
3, 6, 12, and 24 hours after the administration of **27**. The tumor is circled with a light blue dashed line. **f** *Ex vivo*
fluorescence images and intensities of tumors and major organs at 24 hours after the administration of **27**. K, Li, S,
H, Lu, and T indicate kidneys, liver, spleen, heart, lungs, and tumor, respectively.

Conclusion

In summary, this study demonstrated the potential of N-terminal amino acids as alternative modification targets for
maleimide derivatives. We applied maleimide derivatives for selective N-terminal modification of peptides and
proteins with various N-terminal amino acids via a copper(II)-mediated [3+2] cycloaddition using commercially
available 2-PC (**2a**). Although the reaction rate of a copper(II)-mediated [3+2] cycloaddition is much slower
compared to cysteine modification via Michael addition at pH 7.4 ($k_{obs} = 10^2$—10^3 M^{-1}sec^{-1} and $t_{1/2} \leq 1$ minute), the

experimental procedure is straightforward, involving incubation of all reagents under weakly acidic conditions at pH 6.0 and 37°C for 3-6 hours. The simple experimental procedure involved incubating all reagents under mild conditions at pH 6.0 and 37°C for 3–6 hours. Additionally, the combination with readily accessible azide–2-PC **15** enabled dual functionalization of the N-terminus with artificial molecules in a stepwise manner. This developed methodology allowed the construction of modified proteins using click chemistry handles, and the formation of binary and ternary complexes were cross-linked at their N-termini. We successfully applied N-terminal modification to prepare MMAE–Cy5–trastuzumab, a dually modified antibody–drug conjugate that displayed HER2 recognition activity *in vitro* and *in vivo* and exhibited anti-proliferative activity in 2D- and 3D-cultured HER2-positive cells.

For copper(II)-mediated [3+2] cycloaddition in weakly acidic to neutral aqueous solutions, heteroaromatic aldehydes with the coordination motifs, such as 2-PC (**2a**), were necessary. In conventional metal-mediated [3+2] cycloadditions of amino acid imines with maleimides in organic solvents, the bidentate coordination of amino acid imines with metal ions promotes the formation of azomethine ylides. However, because amino acid imines are vulnerable to hydrolysis, additional coordination from heteroaromatic nitrogen is required to stabilize the imines in aqueous solution. Furthermore, the electron-withdrawing inductive effect of the heteroaromatic ring increases the acidity of the α-proton, presumably allowing the formation of azomethine ylide formation under biocompatible conditions without the addition of strong bases. Heteroaromatic aldehydes also advantageously protect the amino groups of lysine residues transiently during the reaction through copper(II)-imine complex formation, suppressing undesired aza-Michael addition and resulting in high N-terminal selectivity.

Copper(II)-mediated [3+2] cycloaddition may face interference from bio-related molecules that bind copper(II) ions, such as glutathione and metal-binding proteins. This limitation restricts the practical implementation of the method for protein modification in live cells or *in vivo* studies. However, it is applicable to chemical modification of most peptides and expressed proteins *in vitro*, excluding peptides and proteins with acyl groups or metal-binding motifs at the N-terminus. The widespread availability of maleimide derivatives and the simplicity of the procedure enable researchers to apply this methodology across various fields.

Methods

General procedure for copper(II)-mediated N-terminal modification of peptide

Peptide (2 μL, 2.5 mM in H₂O) was incubated with an aldehyde (1 μL, 50 mM in DMSO), a dipolarophile (1 μL, 50 mM in DMSO), and Cu(OAc)₂ (1 μL, 50 mM in H₂O) in phosphate buffer (20 μL, 10 mM, pH 6.0) for a given time of period at 37 °C. The reaction was quenched with EDTA (1 μL, 100 mM in H₂O) and methoxyamine (1 μL, 1 M in H₂O at pH 4.5). The mixture was analyzed by LC-MS (gradient elution: 0–3 min, 5% B; 3–16 min, 5–75% B), LC-MS/MS (gradient elution: 0–3 min, 5% B; 3–19 min, 5–95% B), and MALDI-TOF MS.

Preparation of the modified peptide T 4aa for the structure determination by NMR studies

Peptide T (**1**) (1 mL, 2.5 mM in H₂O) was incubated with **2a** (2.4 μL), **3a** (125 μL, 200 mM in DMSO), and Cu(OAc)₂ (250 μL, 100 mM in H₂O) in phosphate buffer (11.125 mL, 10 mM, pH 6.0) for 3 h at 37 °C. The reaction

was quenched with EDTA (0.5 mL, 100 mM in H_2O). The resulting solution was purified by preparative HPLC (gradient elution: 0–15 min, 15% B. The fractions at 8.5 and 10.2 min were collected and lyophilized to obtain a colorless powder. The powder was dissolved in DMSO-d_6 (600 μL) and analyzed by LC-MS, ^{1}H NMR, ^{13}C NMR, HSQC, HMBC, and TOCSY.

X-ray crystallographic analysis of (±)-5, N-terminal substructure of 4aa

The analysis of (±)-**5** was performed on a diffractometer equipped with a beamline BL-5A at KEK (the High Energy Accelerator Research Organization, Japan) with a Pilatus3 S6M detector (synchrotron, λ = 0.7500 Å, T = 95 K). Using Olex2,[65] the structure was solved with the SHELXT[66] structure solution program using Intrinsic Phasing and refined with the SHELXL[67] refinement package using Least Squares minimization. All non-hydrogen atoms were refined with anisotropic displacement parameters. All hydrogen atoms were created with ideal geometry and refined using a riding model.

Crystallographic data have been deposited with Cambridge Crystallographic Data Centre: Deposition number CCDC-2354963. Copies of the data can be obtained free of charge via http://www.ccdc.cam.ac.uk/conts/retrieving.html (or from the Cambridge Crystallographic Data Centre, 12, Union Road, Cambridge, CB2 1EZ, UK; Fax: +44 1223 336033; e-mail: deposit@ccdc.cam.ac.uk). The single crystal of (±)-**5** was prepared by a vapor diffusion method. (±)-**5** was dissolved in AcOEt. The solution in a micro vial was put into a vial filled with pentane and was stayed overnight. Crystal data of (±)-**5**: $C_{32}H_{40}N_8O_6$, colorless, 0.2 × 0.15 × 0.07 mm^3, orthorhombic, space group Pna2$_1$, a = 19.2530(6), b = 17.0120(6), c = 9.706(2) Å, α = 90°, β = 90°, γ = 90°, V = 3179.0(7) Å^3, ρ_{calcd} = 1.322 g/cm^3 , Z = 4, 11265 unique reflections (R_{int} = 0.0210, R_{sigma} = 0.0136) out of 68265 with I > 2σ (I) reflections measured, R_1 = 0.03883, and wR_2 = 0.1050 [I > 2σ(I)], R_1 = 0.0403, and wR_2 = 0.1068 for all data, GOF = 1.060, and flack parameter = −0.04(9).

Stability test of the modified peptide T 4aa

The modified peptide T **4aa** (10.9 μL, 1.83 mM in DMSO-d_6) was incubated for a given period of time in the following solution (89.1 μL): aqueous HCl solution (0.1 M), phosphate buffer (50 mM, pH 7.4), aqueous NaOH solution (0.1 M), aqueous glutathione (reductive form) solution (1 mM in phosphate buffer (50 mM, pH 7.4)), aqueous TCEP solution (1 mM in phosphate buffer (50 mM, pH 7.4)), or aqueous H_2O_2 solution (1 mM in phosphate buffer (50 mM, pH 7.4)). The reaction mixture was analyzed by LC-MS. The remaining percent of **4aa** was calculated by using the peak area in total ion chromatograms.

N-Terminal protein modification with 2a and 3a

A solution (2 μL) of myoglobin (10 mg/mL in 10 mM phosphate buffer at pH 7.5), lysozyme (10 mg/mL in 10 mM

phosphate buffer at pH 7.5), ubiquitin (10 mg/mL in 10 mM phosphate buffer at pH 7.5), or β-lactoglobulin A (10 mg/mL in 10 mM phosphate buffer at pH 7.5) was incubated with **2a** (1 μL, 50 mM in DMSO), **3a** (1 μL, 50 mM in DMSO) and Cu(OAc)$_2$ (1 μL, 50 mM in H$_2$O) in phosphate buffer (20 μL, 10 mM, pH 6.0) for a given period of time at 37 °C. The reaction was quenched with EDTA (1 μL, 100 mM in H$_2$O) and methoxyamine (1 μL, 1 M in H$_2$O at pH 4.5). The mixture was analyzed by LC-MS. Deconvoluted mass spectrum was obtained using LabSolutions Insight Explore software.

In-gel digestion and MALDI-TOF MS and LC-MS/MS analysis for identification of modification site

The reaction mixture of myoglobin, lysozyme, ubiquitin, or β-lactoglobulin A with **2a** and **3a** was diluted with 2×sample buffer with 2-mercaptoethanol (30566-22, nacalai tesque, INC.) and the resulting mixture was boiled for 5 min. The samples were loaded on a 12% acrylamide gel and run for 50 min at 200 V constant. After CBB staining, each band corresponding to modified proteins was separated. Separated gels were cut into ca. 1-mm cubes. The gel pieces were washed twice with 50% MeCN, 0.1% TFA in H$_2$O. For destaining, the gel pieces were incubated with 50% MeCN in aqueous NH$_4$HCO$_3$ solution (100 mM) for 45 min at 37 °C for de-staining and then in MeCN at room temperature for dehydration. To the tube, 100 mM dithiothreitol in aqueous NH$_4$HCO$_3$ solution (100 mM) was added to reduce disulfide bonds in a protein. The resulting mixture was reacted at 37 °C for 30 min. Freed thiols were capped by incubation with 250 mM iodoacetamide in aqueous NH$_4$HCO$_3$ solution (100 mM) for 30 min at room temperature under dark. The gels were washed sequentially with aqueous NH$_4$HCO$_3$ solution (100 mM), 50% MeCN in aqueous NH$_4$HCO$_3$ solution (100 mM), and MeCN. After drying gels, trypsin gold (Promega) (20 μg/mL in 10% MeCN in aqueous NH$_4$HCO$_3$ solution (40 mM)) was added to dried gels in the tube and the mixture was incubated for 60 min at rt. To the mixture, 10% MeCN in in aqueous NH$_4$HCO$_3$ was further added and the whole was incubated overnight at 37 °C. The supernatant was collected in a new tube and the gels were washed with H$_2$O and 50% MeCN, 5% TFA in H$_2$O. Liquids were combined and freeze-dried. The residue was redissolved in 0.1% TFA in H$_2$O and desalted and concentrated using ZipTip® C18 to prepare a sample for MALDI-TOF MS.

N-Terminal protein modification with 2-PC derivative and maleimide derivative

A solution (32 μL) of myoglobin (10 mg/mL in 10 mM phosphate buffer at pH 7.5), ubiquitin (10 mg/mL in 10 mM phosphate buffer at pH 7.5), or β-lactoglobulin A (10 mg/mL, 10 mM phosphate buffer at pH 7.5) was incubated with 2-PC **2a** or **15** (16 μL, 50 mM in DMSO), maleimide **17**—**19** (16 μL, 50 mM in DMSO) and Cu(OAc)$_2$ (16 μL, 50 mM in H$_2$O) in phosphate buffer (320 μL, 10 mM, pH 6.0) for 3 h at 37 °C. The reaction was quenched with EDTA (16 μL, 100 mM in H$_2$O) and methoxyamine (16 μL, 1 M in H$_2$O at pH 4.5). The mixture was desalted with Zeba™ spin desalting column 7K MWCO and the filtrate was dialyzed in phosphate buffer (20 mM, pH 7.0) using Slide-A-Lyzer Dialysis Cassette 3.5K MWCO (Thermo Fisher) overnight in a cold room. The adducts were

analyzed by LC-MS. Deconvoluted mass spectrum was obtained using LabSolutions Insight Explore software. The concentration of each adduct was estimated by Bradford protein assay for **23** and UV-Vis spectroscopy for **21** and **22**. The following values were used as molar extinction coefficients (ε) at 280 nm. ubiquitin: 1490; β-lactoglobulin A: 17200; methyltetrazine: 12800. The concentrations of **21**, **22**, and **23** were calculated to be 27.5 μM, 29.5 μM, and 16.4 μM, respectively.

Stepwise preparation of ternary conjugate of N-terminal functionalized proteins

Method A: **21**+**22**, then +**23**

Az–Tet–Lac (**21**) (30 μL, 27.5 μM in 20 mM phosphate buffer at pH 7.0) and DBCO–ubiquitin (**22**) (30 μL, 29.5 μM in 20 mM phosphate buffer at pH 7.0) were incubated for 24 h at room temperature. An aliquot (30 μL) was taken for analysis. To the remaining reaction mixture, TCO–Myo (**23**) (15 μL, 16.4 μM in 20 mM phosphate buffer at pH 7.0) was added, and the mixture was incubated for 15 h at room temperature. The resulting mixture was analyzed by SDS-PAGE and HPLC with a size exclusion column.

Method B: **21**+**23**, then +**22**

Az–Tet–Lac (**21**) (30 μL, 27.5 μM in 20 mM phosphate buffer at pH 7.0) and TCO–Myo (**23**) (30 μL, 16.4 μM in 20 mM phosphate buffer at pH 7.0) were incubated for 15 h at room temperature. An aliquot (30 μL) was taken for analysis. To the remaining reaction mixture, DBCO–ubiquitin (**22**) (15 μL, 29.5 μM in 20 mM phosphate buffer at pH 7.0 was added, and the mixture was incubated for 24 h at room temperature. The resulting mixture was analyzed by SDS-PAGE and HPLC with a size exclusion column.

Preparation of MMAE–Cy5–trastuzumab (27)

Trastuzumab (48 μL, 115 μM in PBS) was incubated with azide–2-PC **15** (12 μL, 50 mM in DMSO), Cu(OAc)$_2$ (12 μL, 50 mM in H$_2$O), and sulfo Cy5–maleimide **19** (36 μL, 50 mM in DMSO) in phosphate buffer (492 μL, 10 mM, pH 6.0) for 3 h at 37 °C. The reaction was quenched with EDTA (24 μL, 100 mM in H$_2$O) and methoxyamine (24 μL, 1 M in H$_2$O at pH 4.5). The mixture was desalted with Zeba^{TM} spin desalting column 40K MWCO (Thermo Fisher) to afford azide–Cy5–trastuzumab. DBCO–PEG3–Glu–Val–Cit–PMB–MMAE **2*** (15 μL, 5 mM in DMSO) was added to the filtrate and the mixture was incubated for 2 h at r.t. The mixture was desalted with Zeba^{TM} spin desalting column 40K MWCO and the filtrate was dialyzed in PBS using Slide-A-Lyzer Dialysis Cassette 10K MWCO (Thermo Fisher) overnight in a cold room. The conjugation of sulfo Cy5 to trastuzumab was confirmed by MALDI-TOF MS after the treatment with TCEP and SDS-PAGE. Drug-to-antibody ratio (DAR) was calculated to

be 3.0 by UV-Vis spectroscopy. For UV-Vis spectroscopy, the following values were used as molar extinction coefficients (ε) of trastuzumab and sulfo Cy5 at 280 nm and 366 nm. Trastuzumab: ε_{280} = 215000; sulfo Cy5: ε_{280} = 7500, ε_{649} = 250000.

Papain digestion of MMAE–Cy5–trastuzumab (27)

Papain (10 μL, 10 mg/mL in phosphate buffer at pH 6.5) was diluted with activation buffer (90 μL, 10 mM EDTA, 10 mM cysteine in PBS). The mixture was incubated for 10 min at 37 °C. A solution of activated papain (10 μL) was added to MMAE–Cy5–trastuzumab (25 μL, 1.38 μM in PBS). The mixture was incubated for 1 h at 37 °C and quenched with aqueous H_2O_2 solution (1 μL, 100 mM). The resulting mixture was incubated for 1 h at 37 °C. For SDS-PAGE, the mixture was diluted with 6×sample buffer (10 μL, 09499-14, nacalai tesque, INC.) and the resulting mixture was boiled for 5 min. The samples (8 μL) were loaded on a 4–12% acrylamide gel and run for 45 min at 200 V constant. After a fluorescence image was obtained, the same gel was stained with CBB stain one (04543-51, Nacalai tesque) in accordance with the supplier's protocol.

Cell culture

NCI-N87 cells, a human gastric adenocarcinoma cell line, and MCF-7 cells, a human breast cancer cell line, were maintained in RPMI-1640 medium and McCoy's 5a medium, respectively. Both media were supplemented with 10% fetal bovine serum, 100 U/mL of penicillin, and 100 mg/mL of streptomycin. The cells were incubated in an atmosphere of 5% CO2 at 37°C.

Immunofluorescence experiment

NCI-N87 cells and MCF-7 cells were seeded in μ-Dish (φ = 35 mm; ibidi, Germany) at a cell density of 10,000 cells/dish and cultured overnight. After removing the medium, the cells were washed with PBS and fixed with 4% paraformaldehyde for 10 min at room temperature and pH 7.4. After washing with PBS three times, the cells were blocked in 3% bovine serum albumin solution (in PBS) at room temperature for 30 min. The blocking solution was removed, and the cells were incubated with 100 nM MMAE–Cy5–trastuzumab and 1% DAPI in 3% bovine serum albumin solution at room temperature for 1 hour. The cells were washed with PBS three times, and then fluorescence images were obtained using an FV1000 confocal laser scanning biological microscope (Olympus, Japan). ImageJ software was used to generate images suitable for publication.

Cytotoxicity assay in 2D- and 3D-cultured model

The NCI-N87 (HER2 positive, 25,000 cells/well) and MCF-7 cells (HER2 negative, 3,000 cells/well) were seeded in a 96-well cell culture plate overnight. Thereafter, the cells were treated with either MMAE (0, 0.001, 0.01, 0.1, 1, 2.5, 5, 10, 50, and 100 nM), trastuzumab (0, 0.00035, 0.0035, 0.035, 0.35, 0.875, 1.75, 3.5, 17.5, and 35 nM), or **27** (MMAE [trastuzumab]: 0 [0], 0.001 [0.00035], 0.01 [0.0035], 0.1 [0.035], 1 [0.35], 2.5 [0.875], 5 [1.75], 10 [3.5], 50 [17.5], and 100 [35] nM) for 72 h. Cell viability was determined using a cell count reagent (nacalai tesque, Japan).

To prepare NCI-N87 spheroids, NCI-N87 cells (2.5×10^3 cells/well) were prepared by a liquid overlay method using an ultralow attachment 96-well cell culture plate at 37°C for 96 h.[68] Thereafter, either MMAE (0, 0.1, 1, 10, and 100 nM), trastuzumab (0, 0.035, 0.35, 3.5, and 35 nM), or **27** (MMAE [trastuzumab]: 0 [0], 0.1 [0.035], 1 [0.35], 10 [3.5], and 100 [35] nM) was added to spheroids (final concentration: 0, 0.1 1, 10, and 100 nM), and further incubated at 37°C for 72 h. The image of spheroid morphology using a phase-contrast microscope (BZ-X700).

Confocal microscopy

NCI-N87 cells (10,000 cells/dish) and MCF-7 cells (10,000 cells/dish) were cultured in μ-Dish (ibidi, Germany) overnight. After washing with PBS thrice, cells were fixed with 10% paraformaldehyde at room temperature for 10 min. The cells were washed with PBS thrice and blocked in PBS containing 3% bovine serum albumin at room temperature for 30 min. The blocking solution was removed, and the cells were incubated with 100 nM MMAE–Cy5–trastuzumab **27** with 1% DAPI in 3% bovine serum albumin solution at room temperature for 1 h. The cells were washed with PBS thrice, then fluorescence images were obtained by FV3000 confocal laser scanning biological microscope (Olympus, Japan).

Biodistribution experiment in NCI-N87 tumor-bearing mice

After acclimation for one-week, five BALB/c Slc-nu/nu mice (7-week-old females, Japan SLC, Inc., Shizuoka, Japan) were subcutaneously inoculated NCI-N87 cells (1.5×10^7 cells/mouse) on the back of the right femoral area. Four NCI-N87 tumor-bearing mice (tumor size: 169 ± 42 mm3) were intravenously received MMAE–Cy5–trastuzumab **27** (0.22 mg/kg, 7.5 mL/kg). At 1, 3, 6, 12, and 24 h after injection, the fluorescence intensity of whole body was obtained using IVIS Lumina LT (PerkinElmer Inc., Waltham, MA, USA). After obtaining final whole-body image (24 h), the mice were euthanized by cervical dislocation to harvest biological samples (blood, kidneys, liver, spleen, heart, lungs, and tumor). Fluorescence intensity (Ex/Em = 660/710 nm) in the biological samples were quantitative by IVIS Lumina LT (PerkinElmer Inc., Waltham, MA, USA). The animal experiments were approved by the Institutional Animal Care and Use Committee of Keio University (A2022-123).

Data availability

All data generated or analyzed during this study are included in this published article and its supplementary information files. The additional data that support the findings of this study are available from the corresponding author upon reasonable request.

References

1. Krall, N., da Cruz, F. P., Boutureira, O. & Bernardes, G. J. L. Site-selective protein-modification chemistry for basic biology and drug development. *Nat. Chem.* **8**, 103–113 (2016).

2. Hoyt, E. A., Cal, P. M. S. D., Oliveira, B. L. & Bernardes, G. J. L. Contemporary approaches to site-selective protein modification. *Nat. Rev. Chem.* **3**, 147–171 (2019).

3. Shadish, J. A. & DeForest, C. A. Site-Selective Protein Modification: From Functionalized Proteins to Functional Biomaterials. *Matter* **2**, 50–77 (2020).

4. Ma, N. *et al.* 2H-Azirine-Based Reagents for Chemoselective Bioconjugation at Carboxyl Residues Inside Live Cells. *J. Am. Chem. Soc.* **142**, 6051–6059 (2020).

5. Hahm, H. S. *et al.* Global targeting of functional tyrosines using sulfur-triazole exchange chemistry. *Nat. Chem. Biol.* **16**, 150–159 (2020).

6. Spradlin, J. N., Zhang, E. & Nomura, D. K. Reimagining Druggability Using Chemoproteomic Platforms. *Acc. Chem. Res.* **54**, 1801–1813 (2021).

7. Fang, H. *et al.* Recent advances in activity-based probes (ABPs) and affinity-based probes (AfBPs) for profiling of enzymes. *Chem. Sci.* **12**, 8288–8310 (2021).

8. Wan, C. *et al.* A pyridinium-based strategy for lysine-selective protein modification and chemoproteomic profiling in live cells. *Chem. Sci.* **15**, 5340–5348 (2024).

9. Bridge, H. N. & Weeks, A. M. Proteome-Derived Peptide Libraries for Deep Specificity Profiling of N-terminal Modification Reagents. *Curr. Protoc.* **3**, e798 (2023).

10. Song, X., Ren, X., Mei, Q., Liu, H. & Huang, H. Advancing In-Depth N-Terminomics Detection with a Cleavable 2-Pyridinecarboxyaldehyde Probe. *J. Am. Chem. Soc.* **146**, 6487–6492 (2024).

11. Tamura, T. & Hamachi, I. Chemistry for Covalent Modification of Endogenous/Native Proteins: From Test Tubes to Complex Biological Systems. *J. Am. Chem. Soc.* **141**, 2782–2799 (2019).

12. Ojima, K. *et al.* Ligand-directed two-step labeling to quantify neuronal glutamate receptor trafficking. *Nat. Commun.* **12**, 831 (2021).

13. Dhanjee, H. H. *et al.* Protein–Protein Cross-Coupling via Palladium–Protein Oxidative Addition Complexes from Cysteine Residues. *J. Am. Chem. Soc.* **142**, 9124–9129 (2020).

14. Taylor, R. J., Geeson, M. B., Journeaux, T. & Bernardes, G. J. L. Chemical and Enzymatic Methods for Post-Translational Protein–Protein Conjugation. *J. Am. Chem. Soc.* **144**, 14404–14419 (2022).

15. Chudasama, V., Maruani, A. & Caddick, S. Recent advances in the construction of antibody–drug conjugates. *Nat. Chem.* **8**, 114–119 (2016).

16. J. Walsh, S. *et al.* Site-selective modification strategies in antibody–drug conjugates. *Chem. Soc. Rev.* **50**, 1305–1353 (2021).

17. Bacauanu, V., Merz, Z. N., Hua, Z. L. & Lang, S. B. Nickel-Catalyzed Antibody Bioconjugation. *J. Am. Chem. Soc.* **145**, 25842–25849 (2023).

18. Vinogradova, E. V., Zhang, C., Spokoyny, A. M., Pentelute, B. L. & Buchwald, S. L. Organometallic palladium reagents for cysteine bioconjugation. *Nature* **526**, 687–691 (2015).

19. Kasper, M.-A. *et al.* Vinylphosphonites for Staudinger-induced chemoselective peptide cyclization and functionalization. *Chem. Sci.* **10**, 6322–6329 (2019).

20. Patel, M. *et al.* The Nitrile Bis-Thiol Bioconjugation Reaction. *J. Am. Chem. Soc.* **146**, 274–280 (2023).

21. Lipka, B. M. *et al.* Ultra-rapid Electrophilic Cysteine Arylation. *J. Am. Chem. Soc.* **145**, 23427–23432 (2023).

22. Doud, E. A. *et al.* Ultrafast Au(III)-Mediated Arylation of Cysteine. *J. Am. Chem. Soc.* **146**, 12365–12374 (2024).

23. Ban, H., Gavrilyuk, J. & Barbas, C. F. Tyrosine Bioconjugation through Aqueous Ene-Type Reactions: A Click-Like Reaction for Tyrosine. *J. Am. Chem. Soc.* **132**, 1523–1525 (2010).

24. Choi, E. J., Jung, D., Kim, J.-S., Lee, Y. & Kim, B. M. Chemoselective Tyrosine Bioconjugation through Sulfate Click Reaction. *Chem. Eur. J.* **24**, 10948–10952 (2018).

25. Alvarez Dorta, D., Deniaud, D., Mével, M. & Gouin, S. G. Tyrosine Conjugation Methods for Protein Labelling. *Chem. Eur. J.* **26**, 14257–14269 (2020).

26. Sato, S. *et al.* Site-Selective Protein Chemical Modification of Exposed Tyrosine Residues Using Tyrosine Click Reaction. *Bioconjugate Chem.* **31**, 1417–1424 (2020).

27. Maruyama, K. *et al.* Protein Modification at Tyrosine with Iminoxyl Radicals. *J. Am. Chem. Soc.* **143**, 19844–19855 (2021).

28. Li, B. X. *et al.* Site-selective tyrosine bioconjugation via photoredox catalysis for native-to-bioorthogonal protein transformation. *Nat. Chem.* **13**, 902–908 (2021).

29. Antos, J. M. & Francis, M. B. Selective Tryptophan Modification with Rhodium Carbenoids in Aqueous Solution. *J. Am. Chem. Soc.* **126**, 10256–10257 (2004).

30. Tower, S. J., Hetcher, W. J., Myers, T. E., Kuehl, N. J. & Taylor, M. T. Selective Modification of Tryptophan Residues in Peptides and Proteins Using a Biomimetic Electron Transfer Process. *J. Am. Chem. Soc.* **142**, 9112–9118 (2020).

31. Hu, J.-J., He, P.-Y. & Li, Y.-M. Chemical modifications of tryptophan residues in peptides and proteins. *J. Pep. Sci.* **27**, e3286 (2021).

32. Nuruzzaman, M. *et al.* Hexafluoroisopropanol as a Bioconjugation Medium of Ultrafast, Tryptophan-Selective Catalysis. *J. Am. Chem. Soc.* **146**, 6773–6783 (2024).

33. Xie, X. *et al.* Oxidative cyclization reagents reveal tryptophan cation–π interactions. *Nature* **627**, 680–687 (2024).

34. Lin, S. *et al.* Redox-based reagents for chemoselective methionine bioconjugation. *Science* **355**, 597–602

(2017).

35. Taylor, M. T., Nelson, J. E., Suero, M. G. & Gaunt, M. J. A protein functionalization platform based on selective reactions at methionine residues. *Nature* **562**, 563 (2018).

36. Kim, J. *et al.* Site-Selective Functionalization of Methionine Residues via Photoredox Catalysis. *J. Am. Chem. Soc.* **142**, 21260–21266 (2020).

37. MacDonald, J. I., Munch, H. K., Moore, T. & Francis, M. B. One-step site-specific modification of native proteins with 2-pyridinecarboxyaldehydes. *Nat. Chem. Biol.* **11**, 326–331 (2015).

38. Wang, S. *et al.* Modification of N-terminal α-amine of proteins via biomimetic ortho-quinone-mediated oxidation. *Nat. Commun.* **12**, 2257 (2021).

39. Bloom, S. *et al.* Decarboxylative alkylation for site-selective bioconjugation of native proteins via oxidation potentials. *Nat. Chem.* **10**, 205–211 (2018).

40. Shandell, M. A., Tan, Z. & Cornish, V. W. Genetic Code Expansion: A Brief History and Perspective. *Biochemistry* **60**, 3455–3469 (2021).

41. Lotze, J., Reinhardt, U., Seitz, O. & Beck-Sickinger, A. G. Peptide-tags for site-specific protein labelling in vitro and in vivo. *Mol. BioSyst.* **12**, 1731–1745 (2016).

42. Martos-Maldonado, M. C. *et al.* Selective N-terminal acylation of peptides and proteins with a Gly-His tag sequence. *Nat. Commun.* **9**, (2018).

43. Dang, B. *et al.* SNAC-tag for sequence-specific chemical protein cleavage. *Nat. Methods* **16**, 319–322 (2019).

44. Guo, M. *et al.* Copper assisted sequence-specific chemical protein conjugation at a single backbone amide. *Nat Commun* **14**, 8063 (2023).

45. Renault, K., Fredy, J. W., Renard, P.-Y. & Sabot, C. Covalent Modification of Biomolecules through Maleimide-Based Labeling Strategies. *Bioconjugate Chem.* **29**, 2497–2513 (2018).

46. Ravasco, J. M. J. M., Faustino, H., Trindade, A. & Gois, P. M. P. Bioconjugation with Maleimides: A Useful Tool for Chemical Biology. *Chem. Eur. J.* **25**, 43–59 (2019).

47. Grigg, R., Kemp, J., Sheldrick, G. & Trotter, J. 1,3-Dipolar cycloaddition reactions of imines of α-amino-acid esters: X-ray crystal and molecular structure of methyl 4-(2-furyl)-2,7-diphenyl-6,8-dioxo-3,7-diazabicyclo[3.3.0]octane-2-carboxylate. *J. Chem. Soc., Chem. Commun.* 109–111 (1978).

48. Grigg, R. & Kemp, J. Pyridoxal-α-amino acid ester aldimines. 1,3-dipolar species of possible biochemical significance. *Tetrahedron Lett.* **19**, 2823–2826 (1978).

49. Adrio, J. & Carretero, J. C. Stereochemical diversity in pyrrolidine synthesis by catalytic asymmetric 1,3-dipolar cycloaddition of azomethine ylides. *Chem. Commun.* **55**, 11979–11991 (2019).

50. Adrio, J. & Carretero, J. C. Recent advances in the catalytic asymmetric 1,3-dipolar cycloaddition of azomethine ylides. *Chem. Commun.* **50**, 12434–12446 (2014).

51. Wei, L., Chang, X. & Wang, C.-J. Catalytic Asymmetric Reactions with *N*-Metallated Azomethine Ylides. *Acc. Chem. Res.* **53**, 1084–1100 (2020).

52. Dubey, S. *et al.* Recent advances in the (3+2) cycloaddition of azomethine ylide. *New J. Chem.* **47**, 8997–9034

(2023).

53. Kumar, S. V. & Guiry, P. J. Catalytic Enantioselective [3+2] Cycloaddition of N-Metalated Azomethine Ylides. *Chem. Eur. J.* **29**, e202300296 (2023).

54. Machida, H. & Kanemoto, K. N-Terminal-Specific Dual Modification of Peptides through Copper-Catalyzed [3+2] Cycloaddition. *Angew. Chem. Int. Ed.* **63**, e202320012 (2024).

55. Wang, C.-J., Liang, G., Xue, Z.-Y. & Gao, F. Highly Enantioselective 1,3-Dipolar Cycloaddition of Azomethine Ylides Catalyzed by Copper(I)/TF-BiphamPhos Complexes. *J. Am. Chem. Soc.* **130**, 17250–17251 (2008).

56. Hanaya, K. *et al.* Single-Step N-Terminal Modification of Proteins via a Bio-Inspired Copper(II)-Mediated Aldol Reaction. *Chem. Eur. J.* **28**, e202201677 (2022).

57. Nájera, C., Retamosa, M. de G. & Sansano, J. M. Recoverable (R)- and (S)-Binap−Ag(I) Complexes for the Enantioselective 1,3-Dipolar Cycloaddition Reaction of Azomethine Ylides. *Org. Lett.* **9**, 4025–4028 (2007).

58. Wang, C.-J., Xue, Z.-Y., Liang, G. & Lu, Z. Highly enantioselective 1,3-dipolar cycloaddition of azomethine ylides catalyzed by AgOAc/TF-BiphamPhos. *Chem. Commun.* 2905–2907 (2009) doi:10.1039/B902556A.

59. Liu, H.-C., Tao, H.-Y., Cong, H. & Wang, C.-J. Silver(I)-Catalyzed Atroposelective Desymmetrization of N-Arylmaleimide via 1,3-Dipolar Cycloaddition of Azomethine Ylides: Access to Octahydropyrrolo[3,4-c]pyrrole Derivatives. *J. Org. Chem.* **81**, 3752–3760 (2016).

60. Wu, Y., Xu, B., Liu, B., Zhang, Z.-M. & Liu, Y. A new trifluoromethylated sulfonamide phosphine ligand for Ag(I)-catalyzed enantioselective [3 + 2] cycloaddition of azomethine ylides. *Org. Biomol. Chem.* **17**, 1395–1401 (2019).

61. Barr, D. A. *et al.* X-Y-ZH Systems as potential 1,3-dipoles: Part 1511Part 14. R. Grigg, H.Q.N. Gunaratne and V. Sridharan, Tetrahedron, 1987, 43, 5887.. Amine generated azaallyl anios versus metallo-1,3-dipoles in cycloadditions of α-amino acid esters. Facile regio- and stereo-specific formation of pyrrolidines. *Tetrahedron* **44**, 557–570 (1988).

62. Kumar, S. V. & Guiry, P. J. Zinc-Catalyzed Enantioselective [3+2] Cycloaddition of Azomethine Ylides Using Planar Chiral [2.2]Paracyclophane-Imidazoline N,O-ligands. *Angew. Chem. Int. Ed.* **61**, e202205516 (2022).

63. Anami, Y. *et al.* Glutamic acid–valine–citrulline linkers ensure stability and efficacy of antibody–drug conjugates in mice. *Nat. Commun.* **9**, 2512 (2018).

64. Lu, H. & Stenzel, M. H. Multicellular Tumor Spheroids (MCTS) as a 3D In Vitro Evaluation Tool of Nanoparticles. *Small* **14**, 1702858 (2018).

65. Dolomanov, O. V., Bourhis, L. J., Gildea, R. J., Howard, J. a. K. & Puschmann, H. OLEX2: a complete structure solution, refinement and analysis program. *J. Appl. Cryst.* **42**, 339–341 (2009).

66. Sheldrick, G. M. SHELXT – Integrated space-group and crystal-structure determination. *Acta Cryst. A* **71**, 3–8 (2015).

67. Sheldrick, G. M. Crystal structure refinement with SHELXL. *Acta Cryst. C* **71**, 3–8 (2015).

68. Okamoto, Y. *et al.* Cell uptake and anti-tumor effect of liposomes containing encapsulated paclitaxel-bound albumin against breast cancer cells in 2D and 3D cultured models. *J. Drug Deliv. Sci. Technol.* **55**, 101381

(2020).

Author contributions

K.H. and S.H. designed the project. K.H. preformed the chemical reactions and interpreted the data. K.T. performed the *in vitro* and *in vivo* studies. Y.W. and M.K. performed X-ray crystallography data collection and analysis. K.H. and S.H. wrote and revised the manuscript.

Competing interests

All authors declare no competing interests.

Additional information

Supplementary information was available.